

## Proton-neutron interactions in $N \approx Z$ nuclei

K. Kaneko<sup>1</sup> and M. Hasegawa<sup>2</sup>

<sup>1</sup>*Department of Physics, Kyushu Sangyo University, Matsukadai, Fukuoka 813-8503, Japan*

<sup>2</sup>*Laboratory of Physics, Fukuoka Dental College, Fukuoka 814-0193, Japan*

(Received 3 December 1998; published 25 June 1999)

Proton-neutron ( $p$ - $n$ ) interactions and their various aspects in  $N \approx Z$  nuclei of  $g_{9/2}$  and  $f_{7/2}$  subshells are studied using a schematic model interaction with four force parameters proposed recently. It is shown that the model interaction reproduces well observed physical quantities: the double differences of binding energies, symmetry energy, Wigner energy, odd-even mass difference, and separation energy, which testifies to the reliability of the model interaction and its  $p$ - $n$  interactions. First of all, the double differences of binding energies are used for probing the  $p$ - $n$  interactions. The analysis reveals different contributions of the isoscalar and isovector  $p$ - $n$  pairing interactions to two types of double differences of binding energies, and also indicates the importance of a unique form of isoscalar  $p$ - $n$  pairing force with all  $J$  components. Next, it is shown that this  $p$ - $n$  force is closely related to the symmetry energy and the Wigner energy. Other calculations demonstrate the significant roles of  $p$ - $n$  interactions in the odd-even mass difference and in the separation energy at  $N = Z$ . [S0556-2813(99)00808-0]

PACS number(s): 21.10.Dr, 21.10.Hw, 21.60.Cs

### I. INTRODUCTION

With the advent of radioactive nuclear beams, the properties of nuclei beyond the proton stability line have attracted experimental and theoretical attention in recent years. Special interest is devoted to a unique aspect originating from the fact that protons and neutrons occupy the same orbits in nuclei with  $N \approx Z$  (see [1] for a review). Consequently, one expects a strong proton-neutron ( $p$ - $n$ ) interaction because of the large spatial overlaps between proton and neutron single-particle wave functions. The correlation energies related to the  $p$ - $n$  interaction have been extracted from the experimental binding energies [2–5]. A double difference of binding energies has been analyzed with the aim of providing input to semiempirical mass formulas [2–4], and with relation to the clustering of nucleons as elementary modes of excitation in nuclei [5]. It has recently been used for study of the  $p$ - $n$  interactions [6,7], and discussed in terms of schematic and realistic shell model calculations [8]. This approach using the double difference of binding energies may provide details of the  $p$ - $n$  interactions, the isoscalar ( $\tau=0$ ) and isovector ( $\tau=1$ )  $p$ - $n$  interactions. The  $p$ - $n$  part of the isovector pairing correlation near  $N=Z$  has been studied in terms of algebraic model [9] and compared with shell model Monte Carlo calculations [10,11]. On the other hand, there are many discussions of the roles of the isoscalar pairing interactions (see Refs. [12–17], for instance).

The experimental data indicate [2–4] that the symmetry energy accompanied by the so-called Wigner energy behaves according to the  $T(T+1)$  dependence ( $T=|T_z|$ ). This form could come from the isospin-invariant Hamiltonian. It has been recently proposed that the Wigner energy originates in the isoscalar pairing interaction [12,13]. They pointed out that the Wigner energy cannot be solely explained in terms of correlations between the  $J=1$  isoscalar  $p$ - $n$  pairs, and the isoscalar  $p$ - $n$  pairs with the other  $J$  contribute significantly [13]. In fact, a recent shell model calculation [18] with the  $J=0$  isovector and  $J=1$  isoscalar pairing forces in the  $N$

$\approx Z$   $fp$  shell nuclei cannot explain the magnitude of the Wigner energy. On the other hand, another paper [19] has discussed the fact that the degeneracy of the  $T=0$  and  $T=1$  states in odd-odd nuclei with  $N=Z$  is produced by a balance of the symmetry energy and the  $J=0$  isovector pairing correlation. The lowering of the  $T=0$  states in  $N=Z$  odd-odd nuclei, according to our investigation [20,21], is caused by a unique form of isoscalar ( $p$ - $n$ ) pairing force including all  $J$  components. This result is consistent with that of Satula *et al.* [12,13]. The unique isoscalar  $p$ - $n$  pairing force, which can be expressed in a simple form including the  $T(T+1)$  term, manifests a close relation to the symmetry energy. We shall discuss this matter by a concrete calculation in this paper.

The odd-even mass difference (OEMD), the extra binding energy of a nucleus relative to its neighbors, is known to be an obvious experimental evidence of the pairing correlation [22]. The pairing phenomena are well understood in terms of the proton-proton ( $p$ - $p$ ) or neutron-neutron ( $n$ - $n$ ) pair condensate, and described by the Bardeen-Cooper-Schrieffer (BCS) theory [23]. The OEMD is often interpreted as a measure of the pairing gap (following the relation  $12/A^{1/2}$  on the average) in medium-heavy and heavy nuclei. The OEMD displays, however, a different feature in  $N \approx Z$  nuclei such as a special increase at  $N=Z$ . An ordinary estimation of the neutron or proton pairing gap from the OEMD is not applicable to these nuclei. On the other hand, it has recently been discussed that the OEMD in light nuclei is affected by deformation as well as  $J=0$  pairing correlation [24–26]. A further investigation of the OEMD should be made in  $N \approx Z$  nuclei. We shall discuss the influence of the  $p$ - $n$  interactions on the OEMD.

The development of recent radioactive nuclear beams facilities provides unstable nuclei beyond the line of proton stability. Experimental and theoretical investigations of proton emitters are increasing. Such phenomena allow a test of the various models on the proton-rich side. For  $N \approx Z$  nuclei,

one can expect that the  $p$ - $n$  interactions also influence the separation energy. Since the  $p$ - $n$  force is considered to be attractive, it might increase the separation energy. In fact, the calculated separation energies by all models without the  $p$ - $n$  interaction are smaller than those of experiments at the  $N = Z$  nuclei.

We need a reliable effective interaction to study the nuclear properties mentioned above. We have proposed an extension of the  $P + QQ$  model with four forces [21], which reproduces quite well the experimental binding energies and energy spectra in  $N \approx Z$  nuclei of  $g_{9/2}$  and  $f_{7/2}$  subshells. This model interaction including different types of  $p$ - $n$  forces is very suitable for our purpose to study various aspects of the  $p$ - $n$  interactions. The main purpose of this paper is to study the  $p$ - $n$  interactions, analyzing the double differences of binding energies, and to check the validity of our model, examining various quantities such as the symmetry energy, the Wigner energy, the odd-even mass difference, and the separation energy in nuclei near  $N = Z$ .

The paper is organized as follows. In Sec. II, we first review our model proposed in the previous paper. Section III contains the analysis of the double differences of binding energies to probe the  $p$ - $n$  interactions. The symmetry energy and the Wigner energy are discussed in Sec. IV. In Sec. V, the odd-even mass differences are analyzed in detail, and the two-proton separation energies are calculated in Sec. VI. Finally, Sec. VII gives the conclusions.

## II. MODEL INTERACTION

We have proposed the following effective interaction extended from the  $P + QQ$  force which is composed of four isospin-invariant forces (see Ref. [21] in detail):

$$H = H_{\text{sp}} + V_{\text{int}}, \quad (1)$$

$$H_{\text{sp}} = \sum_{\alpha\rho} \epsilon_a c_{\alpha\rho}^\dagger c_{\alpha\rho}, \quad (2)$$

$$V_{\text{int}} = V(P_0) + V(QQ) + V(P_2) + V_{\pi\nu}^{\tau=0}, \quad (3)$$

$$V(P_J) = -\frac{1}{2} g_J \sum_{M\kappa} \sum_{a \leq b} P_{JM1\kappa}^\dagger(ab) \sum_{c \leq d} P_{JM1\kappa}(cd), \quad (4)$$

$$V(QQ) = -\frac{1}{2} \chi : \sum_{\mu} \sum_{ab\rho} Q_{2\mu\rho}^\dagger(ab) \sum_{cd\rho'} Q_{2\mu\rho'}(cd) :, \quad (5)$$

$$V_{\pi\nu}^{\tau=0} = -k^0 \sum_{a \leq b} \sum_{JM} A_{JM00}^\dagger(ab) A_{JM00}(ab), \quad (6)$$

with

$$P_{JM1\kappa}^\dagger(ab) = p_J(ab) A_{JM1\kappa}^\dagger(ab), \quad (7)$$

$$Q_{2\mu\rho}^\dagger(ab) = q(ab) B_{2\mu\rho}^\dagger(ab), \quad (8)$$

$$A_{JM\tau\kappa}^\dagger(ab) = \sum_{m_a m_\beta} \langle j_a m_a j_b m_\beta | JM \rangle \times \sum_{\rho\rho'} \left\langle \frac{1}{2} \rho \frac{1}{2} \rho' \middle| \tau\kappa \right\rangle \frac{c_{\alpha\rho}^\dagger c_{\beta\rho'}}{\sqrt{1 + \delta_{ab}}}, \quad (9)$$

$$B_{2\mu\rho}^\dagger(ab) = \sum_{m_a m_\beta} \langle j_a m_a j_b \bar{m}_\beta | 2\mu \rangle c_{\alpha\rho}^\dagger (-)^{j_b - m_\beta} c_{\beta\rho}, \quad (10)$$

where  $p_0(ab) = \sqrt{(2j_a + 1)\delta_{ab}}$  and  $p_2(ab) = q(ab) = (a \| r^2 Y_2 \| b) / \sqrt{5}$ . We use the notation  $JM$  and  $\tau\kappa$  for the spin and isospin of a nucleon pair, respectively. The subscript  $\rho$  denotes the  $z$  components of isospin  $\pm \frac{1}{2}$ . We also use the notation  $\rho = \pi$  for a proton and  $\rho = \nu$  for a neutron.

Here  $H_{\text{sp}}$  is a single-particle Hamiltonian and  $V_{\text{int}}$  contains the four forces:  $V(P_0)$  stands for the isovector monopole pairing force,  $V(QQ)$  for the isoscalar quadrupole-quadrupole force,  $V(P_2)$  for the isovector quadrupole pairing force, and  $V_{\pi\nu}^{\tau=0}$  for the  $J$ -independent isoscalar  $p$ - $n$  force. The first two forces in the interaction (3) are an extension of the conventional  $P + QQ$  force to the isospin-invariant one. The  $p$ - $n$  part of the monopole and quadrupole pairing forces as well as the  $p$ - $n$  component of the quadrupole-quadrupole force would be important for  $N \approx Z$  nuclei. The last  $p$ - $n$  force is very important for reproducing the experimental binding energy. It is important to note that  $V_{\pi\nu}^{\tau=0}$  can be expressed as a simple form

$$V_{\pi\nu}^{\tau=0} = -\frac{1}{2} k^0 \left\{ \hat{n} \left( \frac{\hat{n}}{2} + 1 \right) - \hat{T}^2 \right\}, \quad (11)$$

where  $\hat{n}$  denotes the total number operator of valence nucleons ( $\hat{n} = \hat{n}_p + \hat{n}_n$ ) and  $\hat{T}$  is the total isospin operator. Our  $p$ - $n$  interaction is composed of four different components and hence is useful in analyzing their respective contributions to various physical quantities.

We applied the above Hamiltonian to examine the binding energies and energy spectra of nuclei with  $A = 82$ – $100$  and  $A = 42$ – $50$  [21]. We adopted only the  $g_{9/2}$  shell for nuclei with  $A = 80$ – $100$  regarding the  $Z = N = 40$  core as inactive, and the  $f_{7/2}$  shell for nuclei with  $A = 40$ – $50$  regarding the  $Z = N = 20$  core as inactive. It may be necessary to extend these model spaces for quantitative discussion. Our calculation itself indicates the insufficiency of the model space  $(f_{7/2})^n$  about energy spectra. We used an extended model space  $(p_{1/2}, g_{9/2})^n$  when comparing calculated energy levels with observed ones in nuclei with  $A \approx 90$ , while experimental data near  $A = 80$  seem to demand a further extension of the model space. The previous paper, however, has shown that the single- $j$  shell model is bearable for semiquantitative discussion about the nuclear binding energy. This simple model makes it possible to clearly see the roles of respective  $p$ - $n$  interactions. We therefore employ the same single- $j$  shell model as that used in Ref. [21], where the following force strengths are used:

$$g_0 = 0.26, \quad X = \chi\{q(g_{9/2}g_{9/2})\}^2 = 1.50,$$

$$G_2 = \frac{1}{2}g_2\{q(g_{9/2}g_{9/2})\}^2 = 0.35,$$

$$k^0 = 0.925 \quad \text{in MeV for the } g_{9/2} \text{ shell region,} \quad (12)$$

$$g_0 = 0.59, \quad X = \chi\{q(f_{7/2}f_{7/2})\}^2 = 1.20,$$

$$G_2 = \frac{1}{2}g_2\{q(f_{7/2}f_{7/2})\}^2 = 0.90,$$

$$k^0 = 1.90 \quad \text{in MeV for the } f_{7/2} \text{ shell region.} \quad (13)$$

Our model with these sets of parameters is considered to be reliable for studying the  $p$ - $n$  interactions in connection with physical quantities related to the binding energy in the  $g_{9/2}$  and  $f_{7/2}$  shell nuclei. The mass dependence of the force parameter  $k^0$  is taken into account in some cases, but it does not change qualitatively the result.

### III. DOUBLE DIFFERENCES OF BINDING ENERGIES AND $p$ - $n$ INTERACTIONS

We define the  $m$ th double difference of binding energies as follows:

$$\delta V^{(m)}(Z, N) = \delta^{(m)}B(Z, N), \quad (14)$$

where  $B(Z, N)$  is the nuclear binding energy. Here the operator  $\delta^{(m)}$  is defined as

$$\begin{aligned} \delta^{(m)}f(Z, N) = & -\frac{1}{m^2}[f(Z, N) - f(Z, N-m) - f(Z-m, N) \\ & + f(Z-m, N-m)]. \end{aligned} \quad (15)$$

The double difference of binding energies,  $\delta V^{(1)}(Z, N)$ , was introduced for investigating the semiempirical mass formula [2–4]. This quantity is expected to roughly represent the  $p$ - $n$  interactions between the last proton and neutron from the form of Eq. (15). Figure 1(a) shows the plot of  $\delta V^{(1)}(Z, N)$  as a function of  $A = N + Z$  for nuclei in the mass region  $A = 16$ –165. Experimental data are taken from Ref. [27]. We see two separate groups in Fig. 1(a), namely, one is for the even- $A$  nuclei (dots) and the other is for the odd- $A$  nuclei (crosses). In both cases, shell effects at  $Z$  or  $N = 28, 40, 50, 82$  are present, while the patterns of dots and crosses are symmetric with respect to the average curve. It is now convenient to divide  $\delta V^{(1)}(Z, N)$  into two parts: the average part of the even- $A$  and odd- $A$  nuclei and the deviation from it. As seen in Fig. 1(a), the former is approximately written as  $I_0 = 40/A$  and the latter has opposite signs for the even- $A$  and odd- $A$  nuclei as follows:

$$\delta V^{(1)}(Z, N) \approx I_0 + (-1)^A I_1. \quad (16)$$

This expression was originally given by de-Shalit [4,28] in the earliest investigations of the effective  $p$ - $n$  interactions. Equation (16) describes the staggering with respect to the

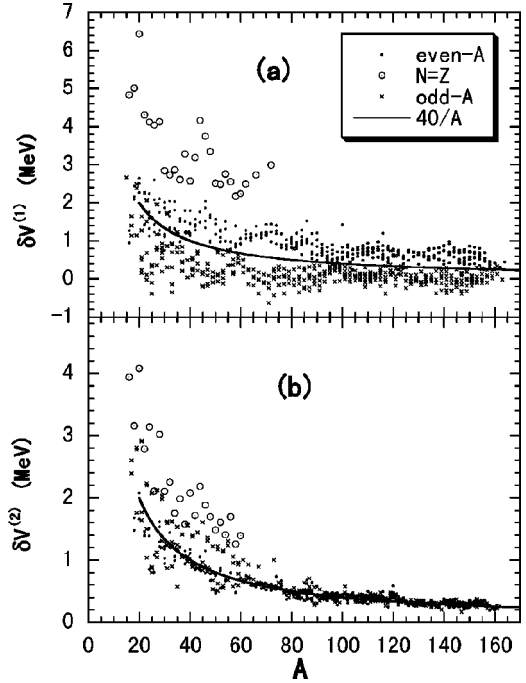


FIG. 1. Plots of the double differences of binding energies derived from the experimental masses in the region  $A = 16$ –164: (a)  $\delta V^{(1)}(Z, N)$  as a function of  $A = N + Z$ , (b)  $\delta V^{(2)}(Z, N)$  as a function of  $A = N + Z$ . The dots stand for even- $A$  nuclei, and the crosses for odd- $A$  nuclei. The curve  $40/A$  is drawn both in (a) and (b).

isotopes for even- $A$  and odd- $A$  nuclei. Large values of  $\delta V^{(1)}(Z, N)$  for even- $A$  nuclei (dots) near  $N = Z$  below  $A = 80$  are notable.

The data of  $\delta V^{(2)}(Z, N)$  are plotted in Fig. 1(b) as a function of  $A = N + Z$ . (Our definition of  $\delta V^{(2)}$  has a sign opposite to that of Brenner *et al.* [8].) The values of  $\delta V^{(2)}$  show a different behavior from  $\delta V^{(1)}$ . It is interesting that the staggering of  $\delta V^{(1)}$  disappears in  $\delta V^{(2)}(Z, N)$ . We see large scatterers of dots and crosses for  $A < 80$ . These correspond to  $\delta V^{(2)}$  of nuclei in  $N \approx Z$ , and the values of  $\delta V^{(2)}$  at  $N = Z$  are especially large. With decreasing mass  $A$ ,  $\delta V^{(2)}$  at  $N = Z$  increases. If one neglects the dots and crosses in  $N \approx Z$  nuclei,  $\delta V^{(2)}$  varies rather smoothly. This smooth trend is clear for  $A > 80$  and continues up to heavy nuclei. This is due to the fact that there is no stable  $N \approx Z$  nuclei with  $A > 80$ . Figure 1(b) clearly indicates the smooth systematic decrease of  $\delta V^{(2)}$  with increasing mass  $A$ , which can be traced by the curve  $40/A$ . The deviations from the curve  $40/A$  are small, and shell structure is not found. This general trend of  $\delta V^{(2)}$  has long been known, and was discussed in several papers. In a recent paper [8], the dramatic spikes of  $\delta V^{(2)}$  at  $N = Z$  light nuclei were discussed in terms of both schematic and realistic shell model calculations, and the importance of  $\tau = 0$   $p$ - $n$  interaction for the spikes was pointed out. The following relationship is derived from Eqs. (14) and (15):

$$\begin{aligned} \delta V^{(2)}(Z, N) = & \frac{1}{4}[\delta V^{(1)}(Z, N) + \delta V^{(1)}(Z, N-1) \\ & + \delta V^{(1)}(Z-1, N) + \delta V^{(1)}(Z-1, N-1)]. \end{aligned} \quad (17)$$

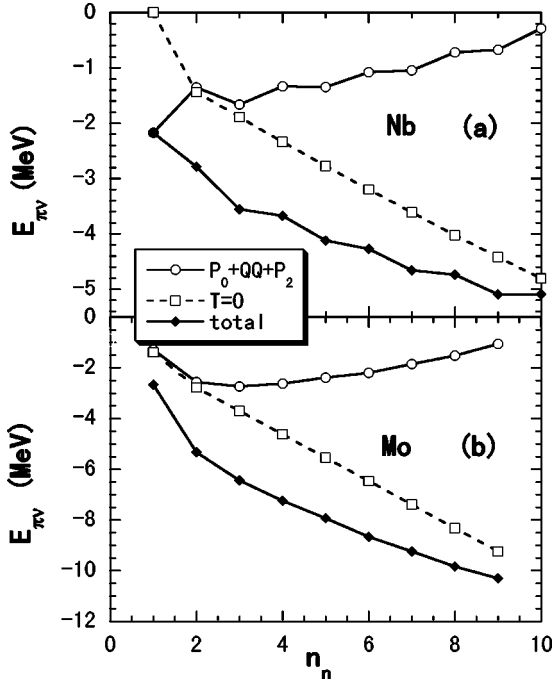


FIG. 2. The calculated  $p$ - $n$  interaction energies as a function of the valence-neutron number  $n_n$  for (a) the Nb isotopes and (b) the Mo isotopes. The open circles stand for the  $p$ - $n$  part of the interaction energy  $E_{\pi\nu}^{P_0+QQ+P_2}$ , the open squares for the  $\tau=0$   $p$ - $n$  interaction energy  $E_{\pi\nu}^{\tau=0}$ , and the diamonds for the total  $p$ - $n$  energy.

Substituting the empirical relationship (16) into Eq. (17), in the large  $A$  limit we get

$$\delta V^{(2)}(Z,N) \approx I_0 = 40/A. \quad (18)$$

Thus, the systematic behavior of  $\delta V^{(2)}(Z,N)$  for  $A > 80$  can be explained from the relation (18). (Strictly speaking, there is a deviation from  $40/A$  due to the mass dependence of  $I_0$ .) Furthermore, it is obtained that  $\delta V^{(m)}(Z,N)$  for  $m=3-6$  have similar pattern to  $V^{(2)}(Z,N)$ , and are also traced by the curve  $40/A$ .

To analyze the double differences of binding energies, we now express the ground-state energy as follows:

$$E(Z,N) = \langle H \rangle = E_{\text{sp}} + E_{\pi\nu}^{P_0+QQ+P_2} + E_{\pi\nu}^{\tau=0} + E_{\pi\pi+\nu\nu}^{P_0+QQ+P_2}, \quad (19)$$

$$E_{\text{sp}} = \langle H_{\text{sp}} \rangle, \quad (20)$$

$$E_{\pi\nu}^{P_0+QQ+P_2} = \langle V_{\pi\nu}^{P_0+QQ+P_2} \rangle, \quad (21)$$

$$E_{\pi\nu}^{\tau=0} = \langle V_{\pi\nu}^{\tau=0} \rangle, \quad (22)$$

$$E_{\pi\pi+\nu\nu}^{P_0+QQ+P_2} = \langle V_{\pi\pi+\nu\nu}^{P_0+QQ+P_2} \rangle, \quad (23)$$

where  $\langle \rangle$  denotes the expectation value with respect to the ground state. Here,  $V_{\pi\nu}^{P_0+QQ+P_2}$  is the  $p$ - $n$  parts of the  $P_0+QQ+P_2$  force, and  $V_{\pi\pi+\nu\nu}^{P_0+QQ+P_2}$  is the proton-proton ( $p$ - $p$ ) and neutron-neutron ( $n$ - $n$ ) parts of the total interaction (3). Figure 2 shows  $E_{\pi\nu}^{P_0+QQ+P_2}$  and  $E_{\pi\nu}^{\tau=0}$  as a function

of valence-neutron number  $n_n$  for Nb and Mo isotopes. The  $p$ - $n$  part of the  $P_0+QQ+P_2$  energy,  $E_{\pi\nu}^{P_0+QQ+P_2}$ , exhibits a characteristic odd-even staggering in Nb isotopes, while  $E_{\pi\nu}^{\tau=0}$  gives a smooth line except for  $n_n=1$ . On the other hand, for Mo isotopes  $E_{\pi\nu}^{P_0+QQ+P_2}$  varies smoothly as  $n_n$  increases, and indicates very different structure from that of Nb isotopes. This can be attributed to extra energy for the odd-odd nuclei, which mainly comes from the  $\tau=1$   $p$ - $n$  part of the  $P_0+QQ+P_2$  force.

Consider the double difference of ground-state energies,  $\delta^{(1)}E(Z,N)$ , using the operator  $\delta^{(1)}$  defined by Eq. (15). Since there are almost no contributions from the single-particle energy  $E_{\text{sp}}$  and Coulomb interaction to the double difference of binding energies as seen in the form of Eq. (15), one notices that  $\delta^{(1)}E(Z,N)$  is able to be compared directly with the experimental value  $\delta V^{(1)}(Z,N)$ . Figure 3 shows the calculated and experimental double differences of binding energies,  $\delta^{(1)}E(Z,N)$  and  $\delta V^{(1)}(Z,N)$ , as a function of mass  $A=N+Z$  for the Nb, Mo, Tc, and Pd isotopes. The Nb and Mo nuclei near  $N=Z$  at the beginning of  $g_{9/2}$  shell region probably have the mixing of single-particle levels, the  $p_{1/2}$ ,  $f_{5/2}$ , and  $p_{3/2}$ . As seen from Figs. 3(a)–3(d), however, the agreement with experiments is quite good. Our calculation reproduces the staggering, and also predicts the highest spikes at  $N=Z$  nuclei though no experimental data are present.

Let us now analyze the staggering and the highest spikes at  $N=Z$ . In Table I, the components of  $\delta^{(1)}E(Z,N)$  for the Mo isotopes are listed. The components  $\delta^{(1)}E_{\pi\nu}^{P_0+QQ+P_2}$ ,  $\delta^{(1)}E_{\pi\nu}^{\tau=0}$ , and  $\delta^{(1)}E_{\pi\pi+\nu\nu}$  are obtained using the definition (15) of the operator  $\delta^{(1)}$  for the respective parts of the ground-state energies, Eqs. (21)–(23). It is seen that the large value at  $N=Z=42$  comes from only the  $\tau=1$  component of  $\delta^{(1)}E_{\pi\nu}^{P_0+QQ+P_2}$ , and others are very small. Thus it is clear that the  $\tau=1$   $p$ - $n$  interaction of the  $P_0+QQ+P_2$  force is closely related to the large values of  $\delta V^{(1)}$  at  $N=Z$ . On the other hand,  $\delta^{(1)}E(Z,N)$  for  $N \neq Z$  exhibits staggering as seen in Table I [also see Fig. 3(b)]. The small values for odd  $N$  are due to the cancellation of  $\tau=1$  and  $\tau=0$  components of  $\delta^{(1)}E(Z,N)$ , and for even  $N$  both  $\tau=1$  and  $\tau=0$  components contribute in phase. The value of  $\delta^{(1)}E_{\pi\nu}^{\tau=0}$  is 0 for  $N=Z$  and  $\frac{1}{2}k^0$  for  $N > Z$ , though the tabulated values have numerical errors.

Figure 4 shows  $\delta^{(2)}E(Z,N)$  and  $\delta V^{(2)}(Z,N)$  as a function of mass  $A=N+Z$  for the Mo, Tc, Pd, and Sn isotopes. The values of  $\delta^{(2)}E(Z,N)$  are a little bit smaller than the experimental ones but the agreement is quite well. Our calculation predicts large  $\delta^{(2)}E(Z,N)$  at  $N=Z$ . The components of  $\delta^{(2)}E(Z,N)$  are shown for the Mo isotopes in Table II. It is seen that  $\delta^{(2)}E(Z,N)$  comes from only the  $\tau=0$   $p$ - $n$  interaction, and the  $\tau=1$  components are small because of the cancellation of  $\delta^{(2)}E_{\pi\nu}^{P_0+QQ+P_2}(Z,N)$  and  $\delta^{(2)}E_{\pi\pi+\nu\nu}(Z,N)$ . The  $\tau=0$  component of  $QQ$  is small except for  $N=42$  and 43. (In other isotopes, this component is small for all  $N$ ; then this behavior for  $N=42,43$  in the Mo isotopes is exceptional.) The value of  $\delta^{(2)}E_{\pi\nu}^{\tau=0}$  is  $3k^0/4$  for  $N=Z$ ,  $5k^0/8$  for  $|N-Z|=1$ , and  $k^0/2$  for  $|N-Z| > 1$ , though the tabulated

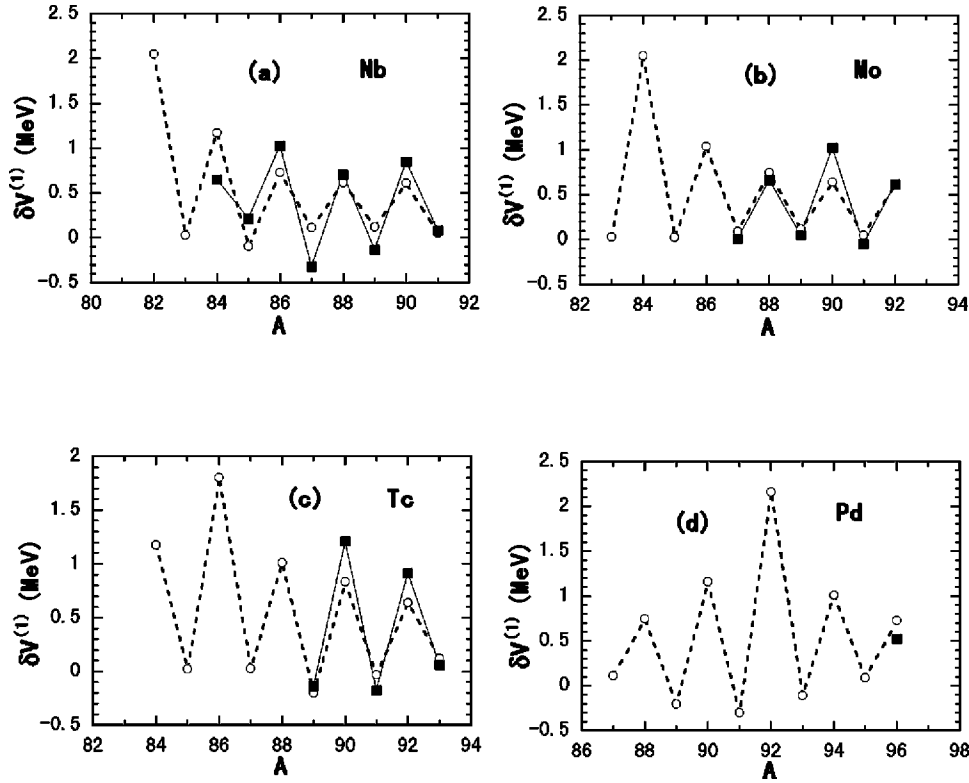


FIG. 3. The calculated values  $\delta^{(1)}E(Z,N)$  (open circles) and the experimental values  $\delta^{(1)}V(Z,N)$  (solid squares) as a function of  $A = N+Z$  for the Nb, Mo, Tc, and Pd isotopes.

values have numerical errors. Thus  $\delta V^{(2)}(Z,N)$  derived from the experimental binding energies are considered to be nearly attributed to the  $\tau=0$   $p$ - $n$  force  $V_{\pi\nu}^{\tau=0}$ . Namely, we deduce an approximate relation

$$\delta V^{(2)}(Z,N) \approx \delta^{(2)}E(Z,N) \approx \delta^{(2)}E_{\pi\nu}^{\tau=0}(Z,N). \quad (24)$$

This is consistent with the argument that  $\delta V^{(2)}(Z,N)$  vanishes if one neglects the  $\tau=0$   $p$ - $n$  interaction in the shell model calculation with a surface  $\delta$  interaction for the  $2s-1d$  shell [8].

TABLE I. The components of  $\delta^{(1)}E(Z,N)$  for the Mo isotopes. The first and second columns denote the  $\tau=1$  components, and the third and fourth columns the  $\tau=0$  components.

$N$	$\tau=1$		$\tau=0$		Total $\delta^{(1)}E$
	$\delta^{(1)}E_{\pi\nu}^{P_0+QQ+P_2}$	$\delta^{(1)}E_{\pi\pi+\nu\nu}$	$\delta^{(1)}E_{\pi\nu}^{QQ}$	$\delta^{(1)}E_{\pi\nu}^{\tau=0}$	
42	2.049	0.001	-0.001	-0.001	2.050
43	-0.602	-0.288	0.451	0.464	0.024
44	0.414	0.398	-0.232	0.460	1.041
45	-0.511	-0.096	0.236	0.461	0.089
46	0.346	0.218	-0.274	0.457	0.747
47	-0.217	-0.004	-0.125	0.463	0.117
48	0.018	0.177	-0.022	0.465	0.638
49	-0.233	0.000	-0.186	0.461	0.047
50	-0.014	0.183	-0.022	0.465	0.611

Furthermore, we calculated  $\delta^{(1)}E(Z,N)$  and  $\delta^{(2)}E(Z,N)$  for the  $1f_{7/2}$  shell nuclei using the shell model  $(f_{7/2})^n$  with the force parameters (13). Figure 5 shows the calculated and experimental double differences of binding energies for the Ti and Cr isotopes. The agreement with experiments is very good. Our effective interaction  $(P_0+QQ+P_2+V_{\pi\nu}^{\tau=0})$  reproduces well the experimental values of the double differences of binding energies also in the  $1f_{7/2}$  shell region. This supports our model Hamiltonian being applicable to a wide range of nuclei. The good agreement tells us that the results in the  $g_{9/2}$  shell region are reliable and give good predictions. It should be also noted that the approximate relation, Eq. (24), holds in this  $1f_{7/2}$  shell region.

It is now meaningful that the  $p$ - $n$  correlation energy  $E_{\pi\nu}^{\tau=0}$  is expressed as

$$E_{\pi\nu}^{\tau=0} = -\frac{1}{2}k^0 \left\{ \frac{n}{2} \left( \frac{n}{2} + 1 \right) - T(T+1) \right\}, \quad (25)$$

for states with the total valence-nucleon number  $n$  and total isospin  $T$  from Eq. (6). For  $N-Z > 1$ , we can easily show that

$$\delta^{(2)}E_{\pi\nu}^{\tau=0} = \frac{k^0}{2}. \quad (26)$$

The global behavior of  $\delta V^{(2)}(Z,N)$  depending on  $40/A$  as seen in Fig. 1(b) combined with the relations (24) and (26) suggests that in a wide-range view the force strength  $k^0$  might have  $1/A$  dependence

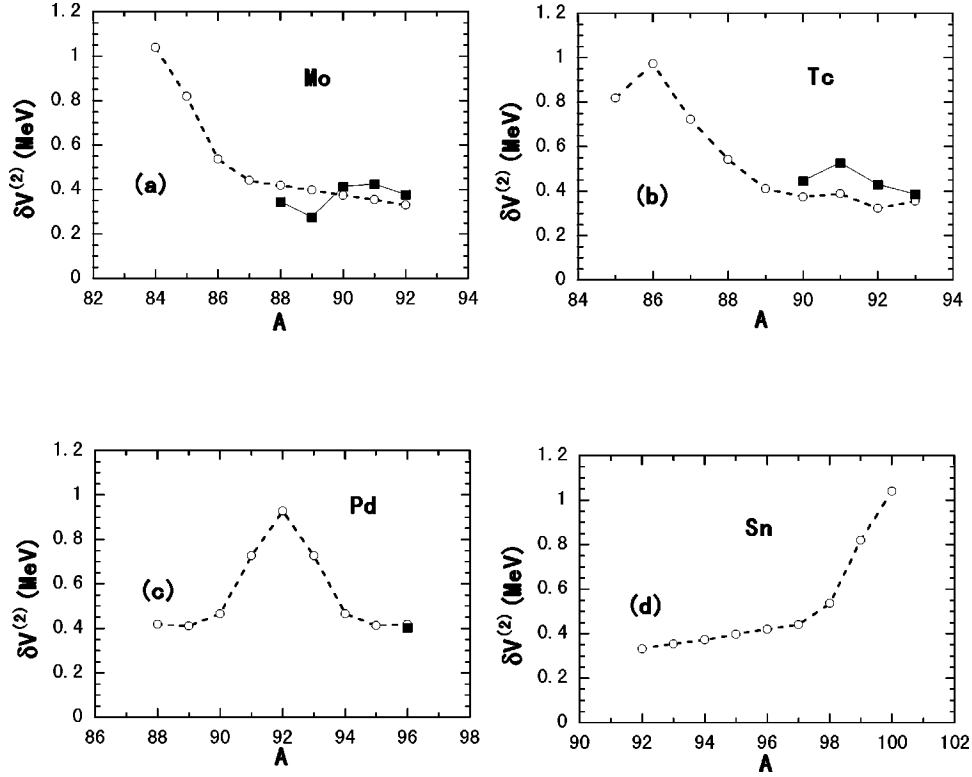


FIG. 4. The calculated values  $\delta^{(2)}E(Z,N)$  (open circles) and the experimental values  $\delta^{(2)}V(Z,N)$  (solid squares) as a function of  $A = N+Z$  for the Mo, Tc, Pd, and Sn isotopes.

$$k^0 \approx \frac{80}{A}. \quad (27)$$

(Strictly speaking, since the double difference  $\delta^{(2)}E_{\pi\nu}^{\tau=0}$  with  $k^0=80/A$  deviates from the curve  $40/A$ , we need a higher-order correction with  $1/A^{4/3}$  to reproduce the curve  $40/A$ .) In fact, the force parameters  $k^0$  employed, 0.925 MeV for the  $1g_{9/2}$  shell nuclei and 1.9 MeV for the  $1f_{7/2}$  shell nuclei, reflect some  $A$  dependence. These values do not very deviate from the global value  $80/A$ , if we compare them with the examples  $80/A=0.93$  for  $A=86$  and  $80/A=1.74$  for  $A=46$ . Certainly, if we impose the  $1/A$  dependence on  $k^0$  like  $1.9 \times (48/A)$  in the calculations for the  $1f_{7/2}$  shell nuclei, the binding energies obtained for  $N \approx Z$  nuclei are reproduced

TABLE II. The components of  $\delta^{(2)}E(Z,N)$  for the Mo isotope.

$N$	$\tau=0$		$\tau=1$		Total $\delta^{(2)}E$
	$\delta^{(2)}E_{\pi\nu}^{QQ}$	$\delta^{(2)}E_{\pi\nu}^{\tau=0}$	$\delta^{(2)}E_{\pi\nu}^{P_0+QQ+P_2}$	$\delta^{(2)}E_{\pi\nu+\nu\nu}$	
42	0.275	0.694	0.365	-0.295	1.039
43	0.237	0.578	0.128	-0.125	0.819
44	0.110	0.462	-0.094	0.058	0.536
45	-0.006	0.462	-0.083	0.069	0.441
46	-0.021	0.461	-0.083	0.063	0.419
47	-0.042	0.461	-0.092	0.070	0.397
48	-0.072	0.463	-0.099	0.080	0.373
49	-0.088	0.463	-0.110	0.089	0.355
50	-0.105	0.464	-0.123	0.094	0.331

better [21]. This improves the double difference of the binding energies  $\delta E^{(2)}(Z,N)$  as seen in Fig. 5, where the circles stand for the constant  $k^0$  and the crosses for the  $k^0=1.9 \times (48/A)$ . Accordingly, the observed variation  $40/A$  in  $\delta V^{(2)}(Z,N)$  is suggested to be mainly attributed to the global dependence  $80/A$  on  $k^0$ . The  $\tau=0$   $p$ - $n$  force  $V_{\pi\nu}^{\tau=0}$  is possibly applicable to  $N > Z$  nuclei with  $T=T_z=(N-Z)/2$ . If it is true, the relation (26) holds for  $N > Z$  too. The  $p$ - $n$  force  $V_{\pi\nu}^{\tau=0}$  with the global parameter  $k^0=80/A$  (with correction) may explain the smooth systematic behavior of  $\delta V^{(2)}(Z,N)$  in the mass region  $A > 80$  as seen in Fig. 1(b). This must be examined further. So far, we have not adopted the  $A$  dependence for the  $P_0$ ,  $QQ$ , and  $P_2$  forces, because we do not have any strong demand to do so within the present calculations in a very tiny model space using a single- $j$  shell. It must, however, be necessary for our model when we make quantitative calculations in many- $j$  shells.

#### IV. SYMMETRY ENERGY AND WIGNER ENERGY

Let us next discuss the symmetry energy  $E_{\text{sym}}=a_{\text{sym}}(N-Z)^2/A$  and Wigner energy  $E_W$  using the same set of parameters as in the previous sections. The experimental data indicate that the symmetry energy accompanied by the Wigner energy is proportional to the  $T(T+1)$  where  $T=T_z=|N-Z|/2$ . Since  $E_{\pi\nu}^{\tau=0}$  includes the  $T(T+1)$  term as seen in Eq. (25), both quantities must be closely related to the isoscalar  $p$ - $n$  force  $V_{\pi\nu}^{\tau=0}$ . Figure 6 shows the symmetry energy coefficient  $a(A)=4a_{\text{sym}}$  in the expression  $E_{\text{sym}}+E_W=a(A)T(T+1)/A$  for the  $f_{7/2}$  shell nuclei. The symmetry

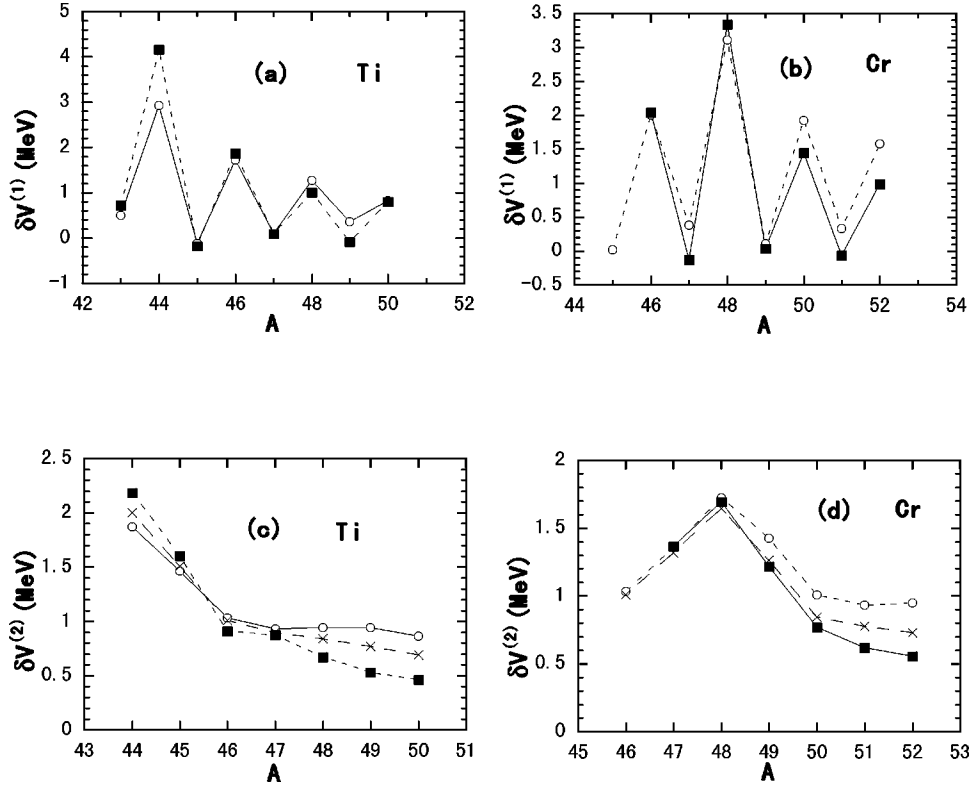


FIG. 5. The double differences of binding energies for the Ti and Cr isotopes, shown in the same manner as Figs. 3 and 4. The solid squares denote the experimental values, and the open circles and crosses denote the calculated values with  $k^0=1.9$  and  $k^0=1.9 \times (48/A)$ , respectively.

energy coefficient can be extracted by the treatment of Jänecke and Comay [29,30]. We calculated the Coulomb-energy-corrected binding energies  $B^* = B(\text{exp}) + E_{\text{Coul}}(\text{cal})$  following Cairier *et al.* [31]. The calculated symmetry energy coefficients nicely reproduce the experimental data in Fig. 6. Where does the symmetry energy come from? We should now analyze the result obtained. If  $V(QQ)$  and  $V(P_2)$  are eliminated from the total Hamiltonian, the Hamiltonian  $H_{\text{sp}} + V(P_0) + V_{\pi\nu}^{\tau=0}$  has  $SO(5)$  symmetry in the

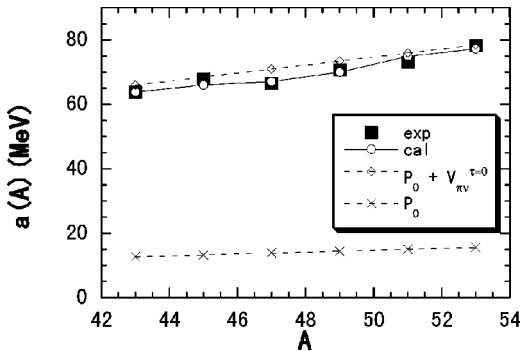


FIG. 6. The symmetry energy coefficients  $a(A)$  in the  $f_{7/2}$  shell region. The calculated and experimental values are denoted by the open circles and solid squares, respectively. The diamonds represent  $\tilde{a}(A) = 1.245A$  in the  $J=0$  isovector plus  $J=\text{odd}$  isoscalar pairing force model, and the crosses  $\tilde{a}(A) = 0.295A$  in the  $J=0$  isovector pairing force model.

single- $j$  shell approximation. The total energy of  $H_{\text{sp}} + V(P_0) + V_{\pi\nu}^{\tau=0}$  in the single- $j$  shell is specified by the total valence nucleon number  $n = n_p + n_n$  and the total isospin  $T$  as follows [9]:

$$\begin{aligned} \tilde{E} &= E_{\text{sp}} + E_{P_0} + E_{\pi\nu}^{\tau=0} \\ &= \epsilon n - \frac{1}{2} \left\{ g_0 n \left( \Omega - \frac{n-6}{4} \right) + k^0 \frac{n}{2} \left( \frac{n}{2} + 1 \right) \right\} \\ &\quad + \frac{1}{2} (g_0 + k^0) T(T+1), \end{aligned} \quad (28)$$

where  $E_{\text{sp}}$ ,  $E_{P_0}$ , and  $E_{\pi\nu}^{\tau=0}$  denote the expectation values of  $H_{\text{sp}}$ ,  $V(P_0)$  and  $V_{\pi\nu}^{\tau=0}$  with respect to ground states with  $n$  and  $T$ , respectively. From the coefficient of the  $T(T+1)$  part in Eq. (28), the symmetry energy coefficient  $\tilde{a}(A)$  is expressed as

$$\tilde{a}(A) = \frac{1}{2} (g_0 + k^0) A, \quad (29)$$

which is proportional to the sum of the force strengths  $g_0$  and  $k^0$ . The parameter set (12) gives the value  $\tilde{a}(A) = 1.245A$  in the  $f_{7/2}$  region. As shown in Fig. 6, the symmetry energy coefficient  $\tilde{a}(A)$  almost describes that obtained with the total Hamiltonian including  $V(QQ)$  and  $V(P_2)$ .

Thus, we see that the symmetry energy in this region originates in the isoscalar  $p$ - $n$  force  $V_{\pi\nu}^{\tau=0}$  and isovector  $J=0$  pairing force. Their contributions are 76% and 24%, respectively, in the present calculation.

In the expression  $E_{\text{sym}} + E_W = a(A)T(T+1)/A$ , the Wigner energy has the same coefficient as the symmetry energy, and is expressed as  $E_W = a(A)T/A$ . Poves and Martínez-Pinedo pointed out that a shell model calculation with the  $J=0$  isovector pairing force and  $J=1$  isoscalar pairing force in the  $N \approx Z$   $fp$  shell nuclei cannot explain the magnitude of the experimental Wigner energy [18]. If we take the same parameter  $g_0 = 0.295$  for the  $J=0$  isovector pairing force as that of Ref. [18], the Wigner energy is estimated as  $E_W = g_0|N-Z|/4 = 3.54|N-Z|/A$  MeV for  $A=48$ . This value is not very different from the result  $E_W = 3.04|N-Z|/A$  MeV they obtained. The empirical Wigner energy,  $E_W = 47|N-Z|/A$  MeV [13] or  $37|N-Z|/A$  MeV [19,32] is very large compared with these values. Figure 6 tells that the Wigner energy cannot be reproduced without  $V_{\pi\nu}^{\tau=0}$ . If we introduce  $V_{\pi\nu}^{\tau=0}$ , the Wigner energy becomes  $E_W = 37.4|N-Z|/A$  MeV for  $A=60$  from Eq. (29), which is consistent with the empirical formula. We can conclude that the isoscalar  $p$ - $n$  force and isovector  $J=0$  pairing force are origin of both the symmetry energy and Wigner energy. In particular, it is important to note that the isoscalar  $p$ - $n$  interaction with all  $J$  components, not only  $J=1$ , is crucial for reproducing the symmetry energy and the Wigner energy.

## V. ODD-EVEN MASS DIFFERENCE

The odd-even mass difference in three-point and four-point expressions,

$$\Delta_3(Z, N) = \frac{(-1)^N}{2} [B(Z, N+1) - 2B(Z, N) + B(Z, N-1)], \quad (30)$$

$$\Delta_4(Z, N) = \frac{(-1)^N}{4} [B(Z, N+1) - 3B(Z, N) + 3B(Z, N-1) - B(Z, N-2)], \quad (31)$$

is often used to estimate the empirical pairing gap (for neutron) and to determine the pairing force strength. Figure 7 shows the experimental values of  $\Delta_3(Z, N)$  and  $\Delta_4(Z, N)$  as a function of  $N-Z$  in even- $Z$  isotopes with proton number  $Z=20-30$  and 36. In Fig. 7(a),  $\Delta_3(Z, N)$  exhibits a staggering around 1.5 MeV and has a notable peak at  $N=Z$ , while  $\Delta_4(Z, N)$  has a hill near  $N=Z$  and  $N=Z+1$  but varies smoothly for  $N \geq Z+2$ . The OEMD's,  $\Delta_3(Z, N)$  and  $\Delta_4(Z, N)$  are about 1.5 MeV on the average for  $N \geq Z+2$ . This value is usually regarded as a measure of the empirical neutron pairing gap. In addition, we notice the asymmetry of  $\Delta_3(Z, N)$  with respect to  $N-Z=0$ . This may be due to the so-called Nolen-Schiffer anomaly [33], an energy difference between neighboring mirror nuclei, which cannot be explained by the electromagnetic interaction.

The calculated values of  $\Delta_3(Z, N)$  and  $\Delta_4(Z, N)$  are obtained by replacing  $B(Z, N)$  by the ground-state energy

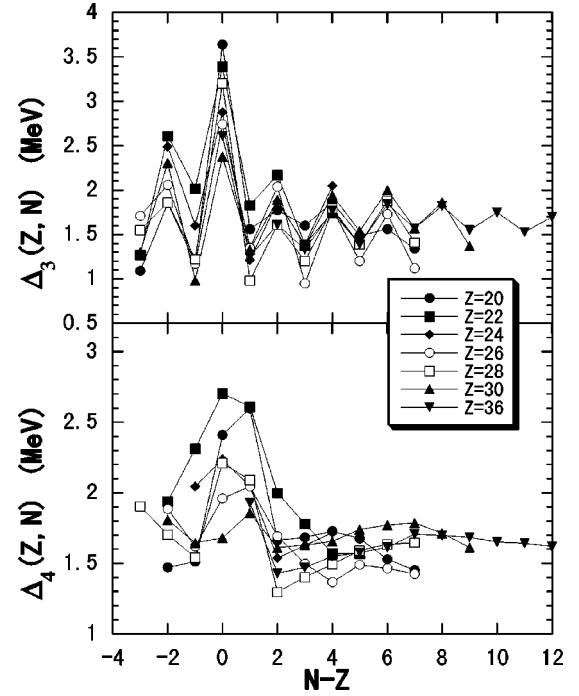
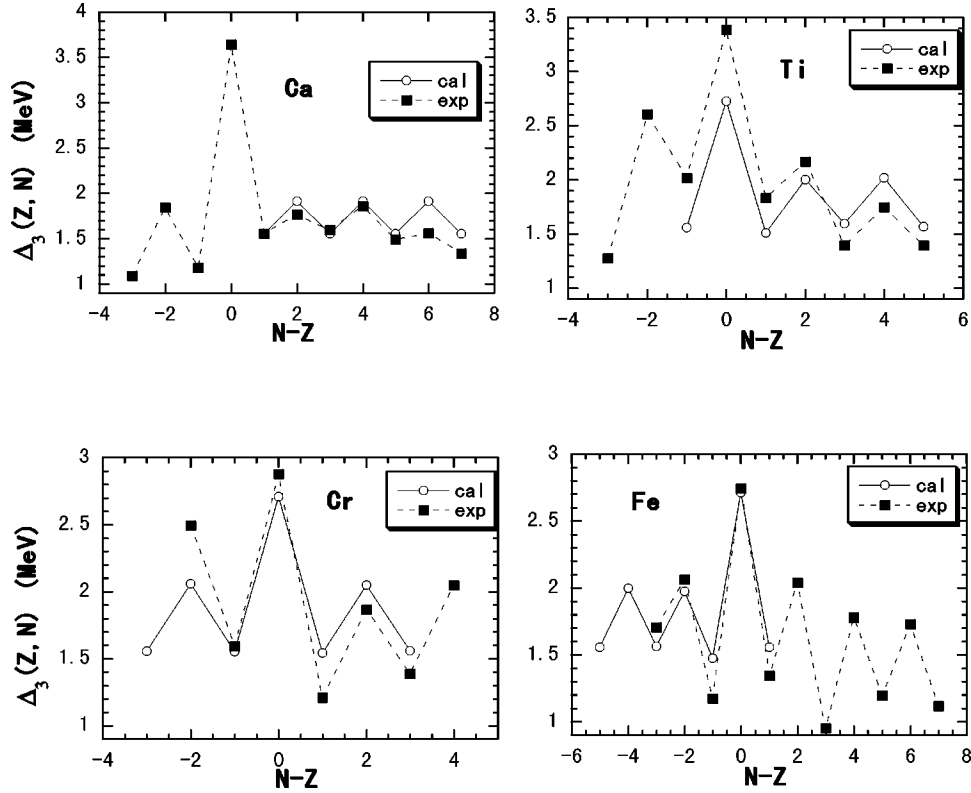


FIG. 7. Dependence of the experimental odd-even mass differences  $\Delta_3(Z, N)$  and  $\Delta_4(Z, N)$  on  $N-Z$  for nuclei with proton number  $Z=20-30$  and 36.

$E(Z, N)$  in Eqs. (30) and (31), since the Coulomb energy hardly contributes to  $\Delta_3(Z, N)$  and  $\Delta_4(Z, N)$ . In our single- $j$  shell model, the single-particle energy has no contribution to  $\Delta_3(Z, N)$  and  $\Delta_4(Z, N)$ . Figure 8 shows the calculated and experimental values of  $\Delta_3(Z, N)$  as a function of  $N-Z$  for the Ca, Ti, Cr, and Fe isotopes. The agreement with experiments is quite good. Especially, the observed peaks at  $N=Z$  are well reproduced.

Let us analyze what interactions are important in  $\Delta_3(Z, N)$ . We separately calculated the contributions of the interaction energies  $E_{\pi\nu}^{P_0+QQ+P_2}$ ,  $E_{\pi\nu}^{\tau=0}$ , and  $E_{\pi\pi+\nu\nu}^{P_0+QQ+P_2}$  to  $\Delta_3(Z, N)$ , and denote them by  $\Delta_{\pi\nu}^{P_0+QQ+P_2}$ ,  $\Delta_{\pi\nu}^{\tau=0}$ , and  $\Delta_{\pi\pi+\nu\nu}^{P_0+QQ+P_2}$ , shortly. In Table III, the components of  $\Delta_3(Z, N)$  are listed for the Cr isotopes. This table indicates the dominance of  $\Delta_{\pi\pi+\nu\nu}^{P_0+QQ+P_2}$ , namely, the dominance of the like-nucleon pairing correlations. The other components of  $\Delta_3(Z, N)$  are very small except that the isovector parts of  $\Delta_{\pi\nu}^{P_0+QQ+P_2}$  and  $\Delta_{\pi\nu}^{\tau=0}$  have large values at  $N=Z$ . We see their additional contributions for the large peaks of  $\Delta_3(Z, N)$  at  $N=Z$  in Fig. 8. The isovector and isoscalar  $p$ - $n$  interactions are most cooperative with the  $p$ - $p$  and  $n$ - $n$  interactions in the  $N=Z$  nuclei.

This situation is explained by illustrating the behavior of the respective interaction energies in Fig. 9. The staggering of  $\Delta_3(Z, N)$  in Fig. 7 is almost attributed to that of  $E_{\pi\pi+\nu\nu}^{P_0+QQ+P_2}$  in Fig. 9. The straight lines of the interaction energies  $E_{\pi\nu}^{P_0+QQ+P_2}$  and  $E_{\pi\nu}^{\tau=0}$  go down as  $N$  increases and turn to the different directions at  $N=Z$ . The coincident ‘‘bends’’ at  $N=Z$  cause the increase (the peak) of  $\Delta_3(Z, N)$  according to the form of Eq. (30). These bends of the  $p$ - $n$


 FIG. 8. The calculated and experimental odd-even mass differences  $\Delta_3(Z, N)$  as a function of  $N-Z$  for the Ca, Ti, Cr, and Fe isotopes.

interaction energies produce the increase of  $\delta V^{(2)}$  around  $N=Z$ . The bends give a special energy gain to the  $N=Z$  even-even nuclei,  $^{44}\text{Ti}$ ,  $^{48}\text{Cr}$ ,  $^{52}\text{Fe}$ , etc. The  $\alpha$ -like four-nucleon correlations in these  $N=Z$  nuclei can be interpreted in terms of the characteristic behavior of the  $p$ - $n$  interactions in cooperation with the like-nucleon interactions [34].

According to Refs. [25,26], on the other hand, the OEMD in light nuclei is strongly affected by deformation originated in the Jahn-Teller mechanism [35]. It is interesting to see what interactions contribute to  $\Delta_{\pi\pi+\nu\nu}^{P_0+QQ+P_2}$  being the main part of  $\Delta_3$ . Table IV presents the respective contributions of the  $P_0$ ,  $QQ$ , and  $P_2$  forces to  $\Delta_{\pi\pi+\nu\nu}^{P_0+QQ+P_2}$  in the Cr isotopes. The dominant component is  $\Delta_{\pi\pi+\nu\nu}^{P_0}$  as expected, i.e., about 2.0 MeV for  $|N-Z| \geq 2$  and about 1.2 MeV for  $N=Z \pm 3$ . In

TABLE III. The components of  $\Delta_3(Z, N)$  for Cr the isotopes. The first and second columns denote the  $\tau=1$  components, and the third and fourth columns the  $\tau=0$  components.

$N$	$\tau=1$		$\tau=0$		Total $\Delta_3(Z, N)$
	$\Delta_{\pi\nu}^{P_0+QQ+P_2}$	$\Delta_{\pi\pi+\nu\nu}^{P_0+QQ+P_2}$	$\Delta_{\pi\nu}^{QQ}$	$\Delta_{\pi\nu}^{\tau=0}$	
21	0.001	1.553	0.002	0.000	1.556
22	-0.027	1.984	0.106	-0.004	2.059
23	0.008	1.657	-0.107	-0.003	1.555
24	0.750	1.500	-0.009	0.469	2.710
25	0.003	1.662	-0.111	-0.013	1.541
26	-0.034	2.007	0.089	-0.015	2.047
27	0.001	1.579	-0.015	-0.005	1.560

addition, there are considerably large contributions of  $\Delta_{\pi\pi+\nu\nu}^{QQ}$  and  $\Delta_{\pi\pi+\nu\nu}^{P_2}$ . Since the  $QQ$  correlation is intimately related to the nuclear deformation, the positive contribution of  $\Delta_{\pi\pi+\nu\nu}^{QQ}$  is consistent with the conclusion of Ref. [26]. The contribution of quadrupole pairing force  $P_2$ , however, is

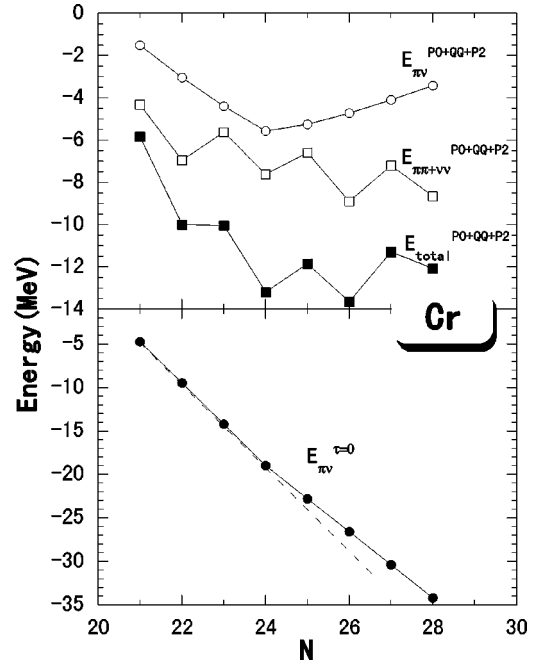

 FIG. 9. Interaction energies of the  $P_0+QQ+P_2$  force and  $V_{\pi\nu}^{\tau=0}$  in the Cr isotopes.

TABLE IV. The components of  $\Delta_{\pi\pi+\nu\nu}^{P_0+QQ+P_2}$  for the Cr isotopes.

$N$	$\Delta_{\pi\pi+\nu\nu}^{P_0}$	$\Delta_{\pi\pi+\nu\nu}^{QQ}$	$\Delta_{\pi\pi+\nu\nu}^{P_2}$	$\Delta_{\pi\pi+\nu\nu}^{P_0+QQ+P_2}$
41	1.182	0.374	-0.003	1.553
42	1.919	0.589	-0.524	1.984
43	2.120	0.279	-0.742	1.657
44	1.901	0.398	-0.799	1.500
45	2.129	0.281	-0.748	1.662
46	1.950	0.594	-0.537	2.007
47	1.211	0.381	-0.013	1.579

negative, and is larger than that of the  $QQ$  correlation for  $|N-Z| \geq 2$ . This is easily understood by the fact that the quadrupole pairing correlation breaks the  $J=0$  Cooper pairs of neutrons. The present calculation tells us that the quadrupole pairing correlation probably cancels the effect of the  $QQ$  correlation or the deformation on the OEMD value [25,26].

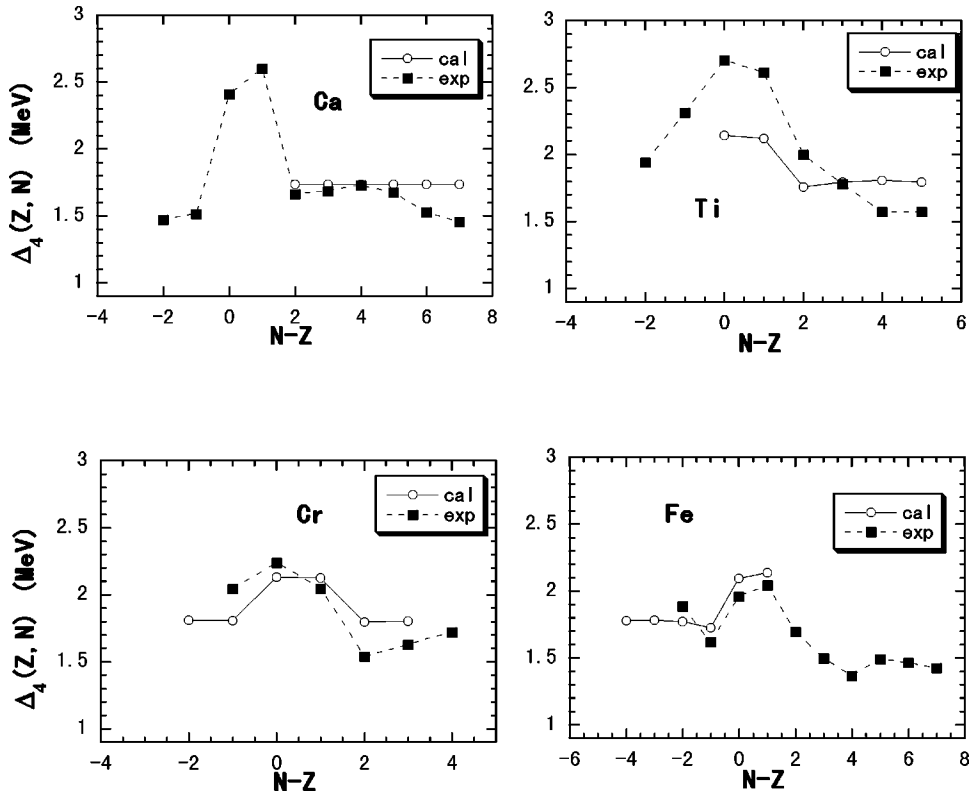
Figure 10 shows calculated and experimental values of  $\Delta_4(Z,N)$  as a function of  $N-Z$  for the Ca, Ti, Cr, and Fe isotopes. The agreement with experiments is quite good except for the Ti isotopes. The calculation reproduces the hill near  $N=Z$  and  $Z+1$  and also the gentle behavior of  $\Delta_4(Z,N)$  near the value 1.6 MeV in the region of  $N>Z+1$  and  $N<Z$ . The increase of  $\Delta_4(Z,N)$  at  $N=Z$  and  $N=Z+1$  is explained in terms of the same mechanism as that of  $\Delta_3(Z,N)$  at  $N=Z$ , which is caused by the coincident bends at  $N=Z$  of the two graphs in Fig. 9 that illustrate the variations of the  $p-n$  interaction energies. The isovector  $p-n$

interactions of the  $P_0+QQ+P_2$  force and the isoscalar  $p-n$  force  $V_{\pi\nu}^{\tau=0}$  are important at  $N=Z$  also for  $\Delta_4(Z,N)$ .

## VI. TWO-PROTON SEPARATION ENERGY

We have investigated several quantities related to the nuclear binding energy in the previous sections. The calculated data include binding energies of nuclei close to the proton drip line. It is interesting to look at the two-proton separation energy, experimental data of which has been accumulated by the radioactive beam. It provides the possibility for studying new decay modes such as diproton emission. Some nuclei around  $^{48}\text{Ni}$  are expected to possibly be two-proton emitters. There is a large deviation between theory and experiment for the two-proton separation energy up to now. All the predictions by the Hartree-Fock (Bogoliubov) and relativistic Hartree-Fock (Bogoliubov) treatments [36,37] underestimate the two-proton separation energies at  $N=Z$  nuclei. This discrepancy could be due to the lack of  $p-n$  interactions in these treatments. As seen in the OEMD in Sec. V, the  $p-n$  correlations cooperate with the  $p-p$  and  $n-n$  correlations especially at  $N=Z$  nuclei. We can expect that the  $p-n$  interactions have a considerable influence on the two-proton separation energy.

We calculated the two-proton separation energies  $S_{2p}$  for the  $f_{7/2}$  shell nuclei with  $Z=20-28$  and  $N=20-28$ . In the calculation, the force strength  $k^0$  is chosen as  $k^0=1.9 \times (48/A)$  which was used in the previous paper [21], because the  $1/A$  dependence of  $k^0$  improves the binding energy and is also supported by the discussion in Sec. III. Calculated val-

FIG. 10. The calculated and experimental odd-even mass differences  $\Delta_4(Z,N)$  as a function of  $N-Z$  for the Ca, Ti, Cr, and Fe isotopes.

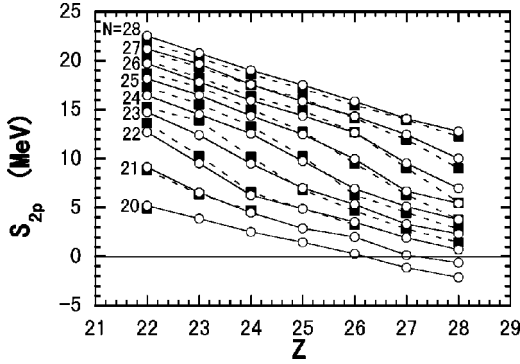


FIG. 11. The two-proton separation energy  $S_{2p}$  in the  $f_{7/2}$  shell region. The calculated and experimental values are denoted by the open circles and solid squares, respectively. The force strength  $k^0$  is taken as  $k^0 = 1.9 \times (48/A)$ .

ues of  $S_{2p}$  are compared with experimental data taken from Ref. [27] in Fig. 11. Here we subtracted the Coulomb energy following Courier *et al.* [31]. The agreement is good. The observed values of  $S_{2p}$  are reproduced well at  $N=Z$  nuclei. Again, the isoscalar  $p$ - $n$  force  $V_{\pi\nu}^{\tau=0}$  plays an important role in the two-proton separation energy at  $N=Z$  as well as in the other quantities discussed above. The model space  $(f_{7/2})^n$  and the set of parameters used are not appropriate for nuclei with large  $Z$  and  $N$ , strictly speaking. According to the experience in this paper, however, the results on the *different quantities of binding energies* might be still meaningful. We note the prediction of our calculation that  $^{48}\text{Ni}$ ,  $^{47}\text{Co}$ , and  $^{49}\text{Ni}$  are possibly unstable,  $^{50}\text{Ni}$  is bound, and  $S_{2p}$  of  $^{46}\text{Fe}$  and  $^{48}\text{Co}$  are close to zero.

## VII. CONCLUSION

We have studied the  $p$ - $n$  interactions using the functional effective interaction with four force parameters which reproduces the energy levels and binding energies of  $N \approx Z$  nuclei considerably well.

First, we analyzed the double differences of binding energies  $\delta V^{(1)}$  and  $\delta V^{(2)}$ , because the two quantities are expected to directly represent the  $p$ - $n$  interactions. Our effective interaction reproduces fairly well the experimental values of  $\delta V^{(1)}$  and  $\delta V^{(2)}$ , and their characteristic behaviors, in the  $g_{9/2}$  and  $f_{7/2}$  shell nuclei. The staggering of  $\delta V^{(1)}$  is due to the competition between  $\tau=1$  and  $\tau=0$  components. The large spike of  $\delta V^{(1)}$  at  $N=Z$  is attributed to the  $\tau=1$   $p$ - $n$  interactions of the  $P_0 + QQ + P_2$  force, and that of

$\delta V^{(2)}$  at  $N=Z$  contrarily represents the  $\tau=0$   $p$ - $n$  interactions. The observed values of  $\delta V^{(2)}$  with respect to mass  $A$  are approximated by the curve  $40/A$ . This curve may be explained by granting an  $A$  dependence on the  $\tau=0$   $p$ - $n$  force strength  $k^0$ .

Second, our effective interaction has also reproduced well the symmetry energy and the Wigner energy for the  $f_{7/2}$  shell nuclei. The strong  $\tau=0$   $p$ - $n$  force  $V_{\pi\nu}^{\tau=0}$  with assistance of the  $\tau=1, J=0$  pairing force is important to explain the magnitudes of the two quantities in this region. It should be noted that the isospin parts of the two forces are proportional to  $T(T+1)$  and their sum is directly related to the symmetry energy in the mass. The  $A$  dependence of the symmetry energy coefficient seems to be determined mainly by that of  $k^0$ .

Third, our effective interaction has described well the observed values of the odd-even mass difference ( $\Delta_3$  and  $\Delta_4$ ) for the  $f_{7/2}$  shell nuclei. The cooperation of the  $p$ - $n$  interactions with the like-nucleon interactions is remarkable at  $N=Z$ . It causes the rise of  $\Delta_3$  and  $\Delta_4$  at  $N=Z$ . The characteristic behaviors of the  $p$ - $n$  interaction energies at  $N=Z$  (see Fig. 9) have an important effect, not only in the double differences of binding energies, but on the odd-even mass difference.

We have briefly touched on the two-proton separation energy  $S_{2p}$  using the calculated binding energies. The calculation indicates a considerably large effect of the  $p$ - $n$  force on  $S_{2p}$  at  $N=Z$ . We noted the prediction of our calculation for  $S_{2p}$  near the  $f_{7/2}$  proton drip line.

The present investigations have shown that the  $p$ - $n$  interactions cause the notable behaviors of the observed quantities related to the binding energy near  $N=Z$  in nuclei where valence protons and neutrons occupy the same shells. Furthermore, our calculations suggest that the  $p$ - $n$  interactions (especially  $V_{\pi\nu}^{\tau=0}$ ) are important for describing these quantities over a wide range of  $N > Z$  nuclei including the neutron drip line.

All the results support the usefulness of the functional effective interaction composed of the four forces  $P_0$ ,  $QQ$ ,  $P_2$ , and  $V_{\pi\nu}^{\tau=0}$ , and clarify the essential roles of  $V_{\pi\nu}^{\tau=0}$  in the physical quantities related to the binding energy. The present calculations, however, have been carried out in the single- $j$  shell model. Calculations in more realistic model spaces are in progress.

## ACKNOWLEDGMENTS

The authors are grateful to J.-Y. Zhang for helpful discussions.

[1] A. L. Goodman, *Adv. Nucl. Phys.* **11**, 263 (1979).  
 [2] J. Jänecke and H. Behrens, *Phys. Rev. C* **9**, 1276 (1974).  
 [3] A. S. Jensen, P. G. Hansen, and B. Jonson, *Nucl. Phys.* **A431**, 393 (1984).  
 [4] J. Jänecke and E. Comay, *Nucl. Phys.* **A436**, 108 (1985).  
 [5] G. G. Dussel, R. J. Liotta, and R. P. J. Perazzo, *Nucl. Phys.* **A388**, 606 (1982).

[6] J.-Y. Zhang, R. F. Casten, and D. S. Brenner, *Phys. Lett. B* **227**, 1 (1989).  
 [7] G. Zaochun and Y. S. Chen, *Phys. Rev. C* **59**, 735 (1999).  
 [8] D. S. Brenner, C. Wesselborg, R. F. Casten, D. D. Warner, and J.-Y. Zhang, *Phys. Lett. B* **243**, 1 (1990).  
 [9] K. T. Hecht, *Phys. Rev.* **139**, B794 (1965); *Nucl. Phys.* **A102**, 11 (1967).

- [10] J. Engel, K. Langanke, and P. Vogel, *Phys. Lett. B* **389**, 211 (1996).
- [11] K. Langanke, D. J. Dean, S. E. Koonin, and P. B. Radha, *Nucl. Phys. A* **613**, 253 (1997).
- [12] W. Satula and R. Wyss, *Phys. Lett. B* **393**, 1 (1997).
- [13] W. Satula, D. J. Dean, J. Gary, S. Mizutori, and W. Nazarewicz, *Phys. Lett. B* **407**, 103 (1997).
- [14] J. Engel, S. Pittel, M. Stoitsov, P. Vogel, and J. Dukelsky, *Phys. Rev. C* **55**, 1781 (1997).
- [15] D. Rudolph *et al.*, *Phys. Rev. Lett.* **76**, 376 (1996).
- [16] D. J. Dean, S. E. Koonin, K. Langanke, and P. B. Radha, *Phys. Lett. B* **399**, 1 (1997).
- [17] K. Kaneko and Jing-ye Zhang, *Phys. Rev. C* **57**, 1732 (1998).
- [18] A. Poves and G. Martínez-Pinedo, *Phys. Lett. B* **430**, 203 (1998).
- [19] P. Vogel, nucl-th/9805015.
- [20] K. Kaneko, M. Hasegawa, and Jing-ye Zhang, *Phys. Rev. C* **59**, 740 (1999).
- [21] M. Hasegawa and K. Kaneko, *Phys. Rev. C* **59**, 1449 (1999).
- [22] A. Bohr, B. R. Mottelson, and D. Pines, *Phys. Rev.* **110**, 936 (1958).
- [23] J. Bardeen, L. N. Cooper, and J. R. Schrieffer, *Phys. Rev.* **108**, 1175 (1957).
- [24] M. Manninen, J. Mansikka-aho, H. Nishioka, and Y. Takahashi, *Z. Phys. D* **31**, 259 (1994).
- [25] H. Häkkinen, J. Kolehmainen, M. Koskinen, P. O. Lipas, and M. Manninen, *Phys. Rev. Lett.* **78**, 1034 (1997).
- [26] W. Satula, J. Dobaczewski, and W. Nazarewicz, *Phys. Rev. Lett.* **81**, 3599 (1998).
- [27] R. B. Firestone and V. S. Shirley, *Table of Isotopes*, 8th ed. (Wiley-Interscience, New York, 1996).
- [28] A. de-Shalit, *Phys. Rev.* **105**, 1528 (1957).
- [29] J. Jänecke and E. Comay, *Nucl. Phys. A* **436**, 108 (1985).
- [30] E. Comay and J. Jänecke, *Nucl. Phys. A* **410**, 103 (1983).
- [31] E. Caurier, P. Zuker, A. Poves, and G. Martínez-Pinedo, *Phys. Rev. C* **50**, 225 (1994).
- [32] J. Duflo and A. P. Zucker, *Phys. Rev. C* **52**, R23 (1995).
- [33] J. A. Nolen and J. P. Schiffer, *Annu. Rev. Nucl. Sci.* **19**, 471 (1969).
- [34] M. Hasegawa, *Prog. Theor. Phys. Suppl.* **132**, 177 (1998).
- [35] W. Nazarewicz, *Nucl. Phys. A* **574**, 27c (1994).
- [36] W. Nazarewicz *et al.*, *Phys. Rev. C* **53**, 740 (1996).
- [37] G. A. Lalazissis and S. Ramman, *Phys. Rev. C* **58**, 1467 (1998).